

Magnetic Fields in Massive Star-forming Regions (MagMaR). V. The Magnetic Field at the Onset of High-mass Star Formation

PATRICIO SANHUEZA,^{1,2,3} JUNHAO LIU (刘峻豪),² KAHU MORII,^{4,2} JOSEP MIQUEL GIRART,^{5,6} QIZHOU ZHANG,⁷ IAN W. STEPHENS,⁸ JAMES M. JACKSON,⁹ PAULO C. CORTÉS,^{10,11} PATRICK M. KOCH,¹² CLAUDIA J. CYGANOWSKI,¹³ PIYALI SAHA,² HENRIK BEUTHER,¹⁴ SUINAN ZHANG (张遂楠),¹⁵ MARIA T. BELTRÁN,¹⁶ YU CHENG,² FERNANDO A. OLGUIN,^{17,2,18} XING LU (吕行),¹⁵ SPANDAN CHOUDHURY,¹⁹ KATE PATTLE,²⁰ MANUEL FERNÁNDEZ-LÓPEZ,²¹ JIHYE HWANG,¹⁹ JI-HYUN KANG,¹⁹ JANIK KAROLY,²⁰ ADAM GINSBURG,²² A. -RAN LYO,¹⁹ KOTOMI TANIGUCHI,² WENYU JIAO,¹⁵ CHAKALI ESWARAIHAH,²³ QIU-YI LUO (罗秋怡),^{15,24,25} JIA-WEI WANG,^{12,26} BENOÎT COMMERÇON,²⁷ SHANGHUO LI,¹⁴ FENGWEI XU,^{28,29,30} HUEI-RU VIVIEN CHEN,¹⁸ LUIS A. ZAPATA,³¹ EUN JUNG CHUNG,¹⁹ FUMITAKA NAKAMURA,^{2,4} SANDHYARANI PANIGRAHY,²³ AND TAKESHI SAKAI³²

¹Department of Earth and Planetary Sciences, Institute of Science Tokyo, Meguro, Tokyo, 152-8551, Japan

²National Astronomical Observatory of Japan, National Institutes of Natural Sciences, 2-21-1 Osawa, Mitaka, Tokyo 181-8588, Japan

³Department of Astronomical Science, SOKENDAI (The Graduate University for Advanced Studies), 2-21-1 Osawa, Mitaka, Tokyo 181-8588, Japan

⁴Department of Astronomy, Graduate School of Science, The University of Tokyo, 7-3-1 Hongo, Bunkyo-ku, Tokyo 113-0033, Japan

⁵Institut de Ciències de l'Espai (ICE, CSIC), Can Magrans s/n, 08193, Cerdanyola del Vallès, Catalonia, Spain

⁶Institut d'Estudis Espacials de Catalunya (IEEC), 08034, Barcelona, Catalonia, Spain

⁷Center for Astrophysics | Harvard & Smithsonian, 60 Garden Street, Cambridge, MA 02138, USA

⁸Department of Earth, Environment, and Physics, Worcester State University, Worcester, MA 01602, USA

⁹Green Bank Observatory, 155 Observatory Rd., Green Bank WV 24944, USA

¹⁰Joint ALMA Observatory, Alonso de Córdova 3107, Vitacura, Santiago, Chile

¹¹National Radio Astronomy Observatory, 520 Edgemont Road, Charlottesville, VA 22903, USA

¹²Academia Sinica, Institute of Astronomy and Astrophysics, No.1, Sec. 4, Roosevelt Rd., Taipei, Taiwan

¹³SUPA, School of Physics and Astronomy, University of St. Andrews, North Haugh, St. Andrews KY16 9SS, UK

¹⁴Max Planck Institute for Astronomy, Königstuhl 17, 69117 Heidelberg, Germany

¹⁵Shanghai Astronomical Observatory, Chinese Academy of Sciences, 80 Nandan Road, Shanghai 200030, People's Republic of China

¹⁶INAF-Osservatorio Astrofisico di Arcetri, Largo E. Fermi 5, I-50125 Firenze, Italy

¹⁷Yukawa Institute for Theoretical Physics, Kyoto University, Kyoto, 606-8502, Japan

¹⁸Institute of Astronomy and Department of Physics, National Tsing Hua University, Hsinchu 300044, Taiwan

¹⁹Korea Astronomy and Space Science Institute (KASI), 776 Daedeokdae-ro, Yuseong-gu, Daejeon 34055, Republic of Korea

²⁰Department of Physics and Astronomy, University College London, Gower Street, London WC1E 6BT, United Kingdom

²¹Instituto Argentino de Radioastronomía (CCT- La Plata, CONICET, CICPBA, UNLP), C.C. No. 5, 1894, Villa Elisa, Buenos Aires, Argentina

²²Department of Astronomy, University of Florida, P.O. Box 112055, Gainesville, FL 32611, USA

²³Department of Physics, Indian Institute of Science Education and Research (IISER) Tirupati, Yerpedu, Tirupati - 517619, Andhra Pradesh, India

²⁴School of Astronomy and Space Sciences, University of Chinese Academy of Sciences, No. 19A Yuquan Road, Beijing 100049, People's Republic of China

²⁵Key Laboratory of Radio Astronomy and Technology, Chinese Academy of Sciences, A20 Datun Road, Chaoyang District, Beijing, 100101, P. R. China

²⁶East Asian Observatory, 660 N. A'ohōkū Place, University Park, Hilo, HI 96720, USA

²⁷Univ. Lyon, Ens de Lyon, Univ. Lyon 1, CNRS, Centre de Recherche Astrophysique de Lyon UMR5574, 69007, Lyon, France

²⁸Kauli Institute for Astronomy and Astrophysics, Peking University, Beijing 100871, People's Republic of China

²⁹I. Physikalisches Institut, Universität zu Köln, Zùlpicher Str. 77, D-50937 Köln, Germany

³⁰Department of Astronomy, School of Physics, Peking University, Beijing, 100871, People's Republic of China

³¹Instituto de Radioastronomía y Astrofísica, Universidad Nacional Autónoma de México, P.O. Box 3-72, 58090, Morelia, Michoacán, México

³²Graduate School of Informatics and Engineering, The University of Electro-Communications, Chofu, Tokyo 182-8585, Japan

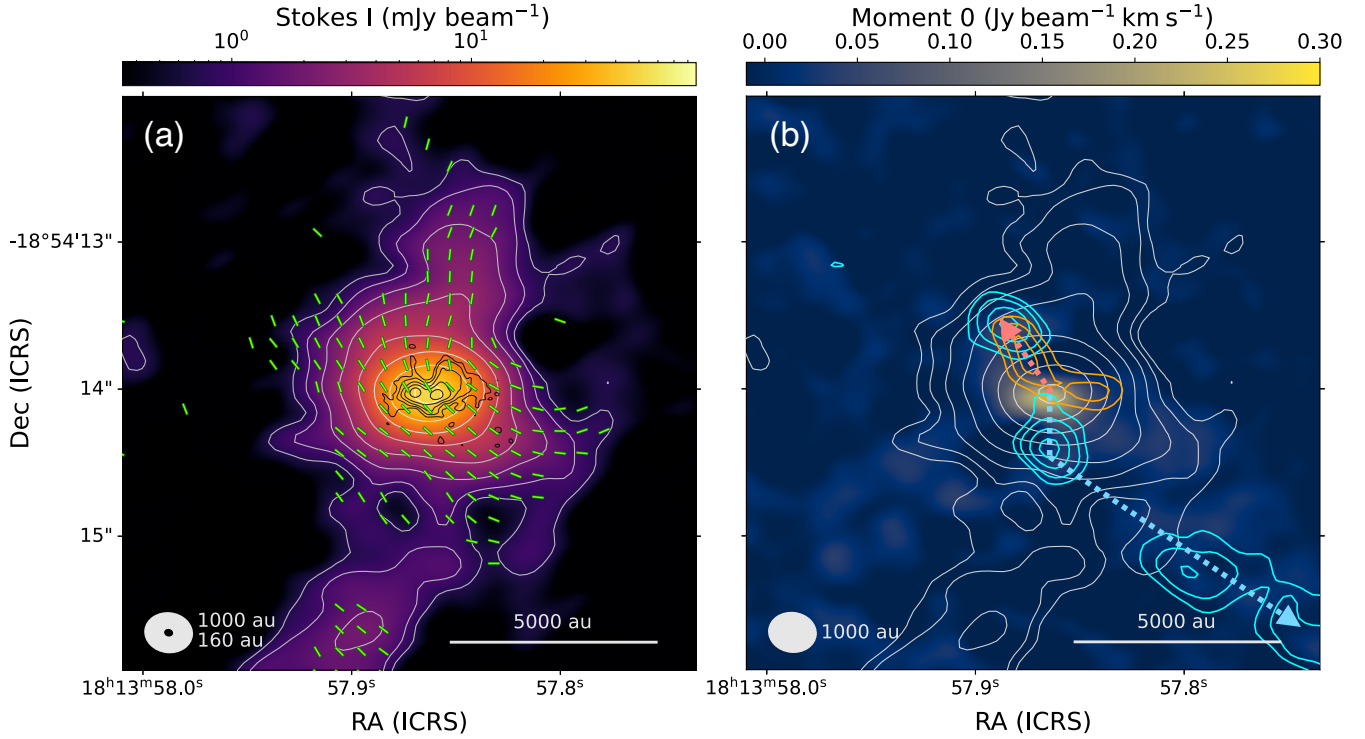


Figure 1. (a) ALMA 1.2 mm dust continuum emission (color scale and white contours) toward G11.92-0.61 MM2 with overlaid magnetic field segments. Green line segments representing the magnetic field orientation (dust polarization vectors rotated by 90 deg, plotted in Nyquist sampling) are plotted above the $3\sigma_{QU}$ level, with $\sigma_{QU} = 30 \mu\text{Jy beam}^{-1}$, and have an arbitrary length. White contours correspond to the dust continuum emission at low resolution ($\sim 0''.3$) in steps of 4, 6, 10, 18, 34, 66, 130, and 258 times the σ_I (rms) value of $181 \mu\text{Jy beam}^{-1}$. Black contours correspond to the 1.33 mm dust continuum emission at high-angular resolution ($\sim 0''.05$) in steps of 5, 10, 20, 40, and 80 times the σ value of $36.1 \mu\text{Jy beam}^{-1}$. (b) Moment 0 map of the $K = 0$ and $K = 1$ transitions combined of CH_3CN ($v = 0, J = 14 - 13$) in color scale. White contours represent the dust continuum emission as in panel (a). Cyan and orange contours correspond to the blueshifted and redshifted outflow emission traced by $\text{CS } J = 5 - 4$ in steps of 3, 5, 8, and 11 times the σ value of $10 \text{ mJy beam}^{-1} \text{ km s}^{-1}$ and in steps of 3, 4, 5, and 6 times the σ value of $4.7 \text{ mJy beam}^{-1} \text{ km s}^{-1}$, respectively. The blueshifted component is integrated from 18 to 32.9 km s^{-1} , and the redshifted component from 41.3 to 44.9 km s^{-1} . The cyan and orange arrows represent the direction of the CH_3OH outflow detected by Cyganowski et al. (2022). The white and black beams at the bottom left represent the spatial resolution of the polarization observations at 1000 au ($0''.3$) and the high-angular resolution observations at 160 au ($0''.05$), respectively. Scale bar is shown on the bottom, right side of each panel.

0, $J = 4$ - 300 m $^{-1}$ pka $^{-1}$ $^{-1}$

66H $^{13}\text{O} + J = 3 - 2$

2 High-resolution Observations

66H $^{13}\text{O} + J = 3 - 2$

66H $^{13}\text{O} + J = 3 - 2$

66H $^{13}\text{O} + J = 3 - 2$

66H $^{13}\text{O} + J = 3 - 2$

66H $^{13}\text{O} + J = 3 - 2$

66H $^{13}\text{O} + J = 3 - 2$

66H $^{13}\text{O} + J = 3 - 2$

66H $^{13}\text{O} + J = 3 - 2$

66H $^{13}\text{O} + J = 3 - 2$

66H $^{13}\text{O} + J = 3 - 2$

66H $^{13}\text{O} + J = 3 - 2$

66H $^{13}\text{O} + J = 3 - 2$

66H $^{13}\text{O} + J = 3 - 2$

66H $^{13}\text{O} + J = 3 - 2$

66H $^{13}\text{O} + J = 3 - 2$

66H $^{13}\text{O} + J = 3 - 2$

66H $^{13}\text{O} + J = 3 - 2$

66H $^{13}\text{O} + J = 3 - 2$

66H $^{13}\text{O} + J = 3 - 2$

66H $^{13}\text{O} + J = 3 - 2$

66H $^{13}\text{O} + J = 3 - 2$

66H $^{13}\text{O} + J = 3 - 2$

66H $^{13}\text{O} + J = 3 - 2$

66H $^{13}\text{O} + J = 3 - 2$

66H $^{13}\text{O} + J = 3 - 2$

66H $^{13}\text{O} + J = 3 - 2$

66H $^{13}\text{O} + J = 3 - 2$

66H $^{13}\text{O} + J = 3 - 2$

66H $^{13}\text{O} + J = 3 - 2$

66H $^{13}\text{O} + J = 3 - 2$

66H $^{13}\text{O} + J = 3 - 2$

66H $^{13}\text{O} + J = 3 - 2$

66H $^{13}\text{O} + J = 3 - 2$

66H $^{13}\text{O} + J = 3 - 2$

66H $^{13}\text{O} + J = 3 - 2$

66H $^{13}\text{O} + J = 3 - 2$

66H $^{13}\text{O} + J = 3 - 2$

66H $^{13}\text{O} + J = 3 - 2$

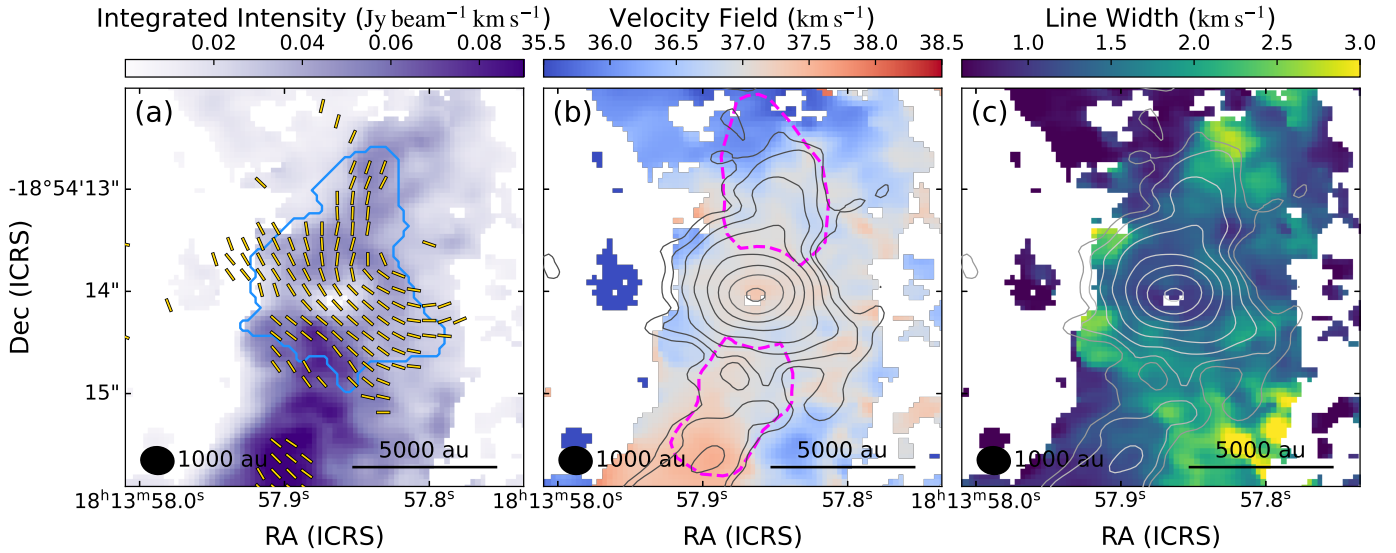


Figure 2. Integrated intensity (a), velocity field (b), and line FWHM (c) obtained from fitting a Gaussian component to the H^{13}CO^+ emission pixel-by-pixel. Contours show the dust continuum emission (same as in Figure 1). All pixels that have a peak intensity, as derived from the Gaussian fitting, larger than 4σ ($\sigma = 3 \text{ mJy beam}^{-1}$) are displayed. In panel (a), the dendrogram from the continuum emission, is displayed in blue (see details in Appendix A.1) and the magnetic field vectors in yellow. Core properties were measured inside the leaf. In panel (b), the areas used to derive the properties of the infalling gas are shown in dashed, magenta masks.

$E_u / \kappa_B > 0.1$
 $J = 4 - 3$
 $K = 0$
 $v_{\text{max},r} = |v_{\text{LSR}}^r - v_{\text{sys}}|$
 $(t_{\text{dyn}} = l_{b,r} / v_{\text{max},b,r})$

$^{13}\text{O} + (J = 3 - 2)$
 $^{13}\text{O} +$
 $^{13}\text{O} +$
 3
 $J = 3 - 2$
 $(E_u / \kappa_B = 2)$

l_b, l_r

$v_{\text{max},b} =$

$v_{\text{max},r} = |v_{\text{LSR}}^r - v_{\text{sys}}|$

$(t_{\text{dyn}} = l_{b,r} / v_{\text{max},b,r})$

¹ The dynamical time scale has not been corrected by the unknown inclination of the outflow. Li et al. (2020) calculate that for a mean inclination angle of $\sim 57.3^\circ$, a correction factor of 0.6 should be applied to t_{dyn} , resulting in dynamical ages of 2700 yr for the blueshifted lobe and 840 yr for the redshifted lobe.

$\rho_{\text{fil}} = \frac{M_{\text{fil}}}{V_{\text{fil}}} = \frac{M_{\text{fil}}}{L_{\text{fil}} \times \pi R_{\text{fil}}^2}$
 $\approx \frac{0.001 M_{\odot}}{0.1 \text{ pc} \times \pi (0.05 \text{ pc})^2} \approx 1.3 \times 10^{-4} M_{\odot} \text{ pc}^{-3}$
 $\approx 1.3 \times 10^{-4} \times 1.5 \times 10^{-6} M_{\odot} \text{ pc}^{-3} \approx 2 \times 10^{-10} M_{\odot} \text{ pc}^{-3}$

4. \mathcal{B}

4 MM2 Core Properties from Dust (Stokes I) and Line Emission

$\rho_{\text{fil}} = \frac{M_{\text{fil}}}{V_{\text{fil}}} = \frac{M_{\text{fil}}}{L_{\text{fil}} \times \pi R_{\text{fil}}^2}$
 $\approx \frac{0.001 M_{\odot}}{0.1 \text{ pc} \times \pi (0.05 \text{ pc})^2} \approx 1.3 \times 10^{-4} M_{\odot} \text{ pc}^{-3}$
 $\approx 1.3 \times 10^{-4} \times 1.5 \times 10^{-6} M_{\odot} \text{ pc}^{-3} \approx 2 \times 10^{-10} M_{\odot} \text{ pc}^{-3}$

$\pm 3 M_{\odot} \pm 3 \times 10^8 \text{ m}^{-3}, \text{ pc}$

$H^{13}O + \dots$
 $M_{\text{fil}} \approx 3 M_{\odot}$
 M_{in}

∇V_{obs}
 σ_{fil}
 $60'' \approx 0.3 \text{ pc}$
 $3 M_{\odot}$

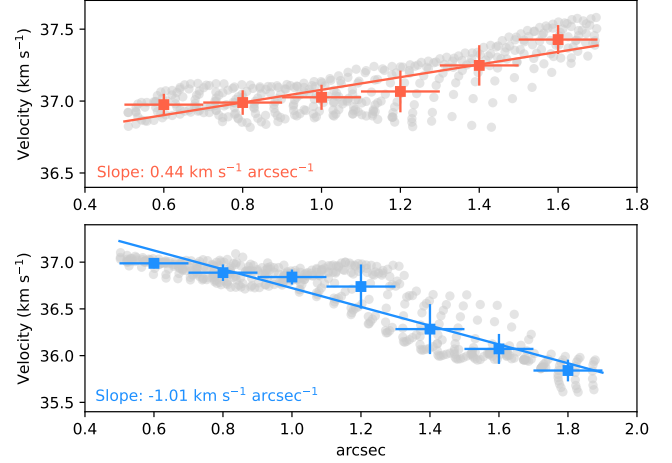


Figure 3. Fitted velocity field to derive the velocity gradient in the filaments. The error bars correspond to the bin width and the standard deviation of the velocities inside each bin for the horizontal and vertical axes, respectively. In the top panel, the velocity gradient of $0.44 \text{ km s}^{-1} \text{ arcsec}^{-1}$ corresponds to $26.9 \text{ km s}^{-1} \text{ pc}^{-1}$, while in the bottom panel the velocity gradient of $1.01 \text{ km s}^{-1} \text{ arcsec}^{-1}$ corresponds to $61.5 \text{ km s}^{-1} \text{ pc}^{-1}$.

2 Mass feeding

$\rho_{\text{fil}} = \frac{M_{\text{fil}}}{V_{\text{fil}}} = \frac{M_{\text{fil}}}{L_{\text{fil}} \times \pi R_{\text{fil}}^2}$
 $\approx \frac{0.001 M_{\odot}}{0.1 \text{ pc} \times \pi (0.05 \text{ pc})^2} \approx 1.3 \times 10^{-4} M_{\odot} \text{ pc}^{-3}$
 $\approx 1.3 \times 10^{-4} \times 1.5 \times 10^{-6} M_{\odot} \text{ pc}^{-3} \approx 2 \times 10^{-10} M_{\odot} \text{ pc}^{-3}$

B

A. ~~13CO~~

A Properties from Dust Continuum Emission

2

 σ_{th} $\sigma_{\text{th}} = \beta \frac{F_{\nu}}{D^2}$

R)

"3000"

$$M = \mathbb{R} \frac{F_{\nu} D^2}{\kappa_{\nu} B_{\nu}(T)},$$

A

$$B_{\nu} = \frac{2 F_{\nu}}{D^2} \frac{1}{\kappa_{\nu}} \frac{1}{\beta} \frac{1}{T} \Rightarrow \beta = \frac{2 F_{\nu}}{D^2 \kappa_{\nu} T} \pm 3 M_{\odot}.$$

$$n(\text{H}_2) = M_{\text{vir}}^{-1} \times \mu_{\text{H}_2} m_{\text{H}} \mu_{\text{H}_2}^{-1}$$

3

$$n(\text{H}_2) \approx \pm 3 \times 10^8 \text{ m}^{-3}.$$

 M_{\odot} ,

A Dynamics and Energetics

$$\sigma_{\text{H}^{13}\text{CO}^+} = \frac{13\text{O} + (V_{\text{H}^{13}\text{CO}^+})^{-1}}{\sigma_{\text{tot}} = \sqrt{\sigma_{\text{th}}^2 + \sigma_{\text{nt}}^2}} \Rightarrow \sqrt{\frac{\pm 0.8}{\sigma_{\text{H}^{13}\text{CO}^+}} \sigma_{\text{th}}^{-1}},$$

$$\sigma_{\text{th}}^2 = \frac{k_{\text{B}} T}{\mu_{\text{p}} m_{\text{H}}}$$

A

$$\sigma_{\text{nt}}^2 = \sigma_{\text{H}^{13}\text{CO}^+}^2 - \frac{k_{\text{B}} T}{m_{\text{H}^{13}\text{CO}^+}},$$

A

$$\mu_{\text{p}} \approx 1.37 m_{\text{H}^{13}\text{CO}^+}$$

$$13\text{O} + \mu_{\text{H}} m_{\text{H}}$$

$$\sigma_{\text{tot}} \approx \pm 0.8 \sigma_{\text{th}}^{-1} \Rightarrow \sigma_{\text{th}} \approx \pm 0$$

$$M = \sigma_{\text{nt}} / \sigma_{\text{th}} \approx \pm 0$$

 α_{vir}

$$M_{\text{vir}} \approx \pm 0$$

² <https://dendrograms.readthedocs.io/en/stable/>

³ <https://almascience.nao.ac.jp/documents-and-tools/cycle11/alma-technical-handbook>

<p> $\alpha_{\text{vir}} < 1$ $E_G < E_K$ </p>	<p> $\alpha_{\text{vir}} > 1$ $E_G > E_K$ </p>
$E_G = -\frac{GM^2}{R} \left(\frac{3-n}{5-2n} \right) \quad \text{and} \quad E_K = \frac{3}{2} M \sigma_{\text{tot}}^2 .$	
$\alpha_{\text{vir}} = \frac{M_{\text{vir}}}{M} \approx \left(\frac{5-2n}{3-n} \right) \frac{R \sigma_{\text{tot}}^2}{GM} ,$	
$\rho(R) \propto R^{-n}; n \approx 1.5$	
<p> $\alpha' < 0.5$ $\alpha' \approx E_{\text{th}}/E_G$ </p>	<p> $\alpha' \beta' < 0.2$ $\beta' \approx E_{\text{rot}}/E_G$ $\sigma_{\text{tot}} \approx \sigma_{\text{th}}$ </p>
$E_{\text{rot}} = \frac{1}{3} M v_{\text{rot}}^2 \left(\frac{3-n}{5-n} \right) ,$	
<p> $v_{\text{rot}} \approx 0.5 \text{ km s}^{-1}$ $\alpha' \beta' \approx \pm 7 \times 10^{-6}$ </p>	<p> $v_{\text{rot}} \approx 1 \text{ km s}^{-1}$ $\alpha' \beta' \approx \pm 2 \times 10^{-3}$ </p>

Table 1. Core Properties at Different Dust Temperatures Excluding the Magnetic Field

T	M	$n(\text{H}_2)$	σ_{th}	σ_{nt}	σ_{tot}	\mathcal{M}	E_G	E_K	E_{th}	E_{rot}	α_{vir}
(K)	(M_{\odot})	(cm^{-3})	(km s^{-1})	(km s^{-1})	(km s^{-1})		(ergs)	(ergs)	(ergs)	(ergs)	
		$\times 10^8$					$\times 10^{46}$	$\times 10^{44}$	$\times 10^{43}$	$\times 10^{43}$	
20	31 ± 13	4.8 ± 2.5	0.26	0.61 ± 0.01	0.66 ± 0.01	2.30 ± 0.03	1.3 ± 1.1	4.0 ± 1.7	6.4 ± 2.7	2.1 ± 0.9	0.060 ± 0.026
50	10 ± 4	1.6 ± 0.8	0.42	0.60 ± 0.01	0.73 ± 0.01	1.44 ± 0.02	0.14 ± 0.12	1.6 ± 0.7	5.2 ± 2.2	0.7 ± 0.3	0.22 ± 0.10

 B. B

$B \approx 0.2 \sqrt{4\pi\rho} \sigma_v \left(\frac{\langle B_t^2 \rangle}{\langle B^2 \rangle} \right)^{-0.5}$

$$B \approx 0.2 \sqrt{4\pi\rho} \sigma_v \left(\frac{\langle B_t^2 \rangle}{\langle B^2 \rangle} \right)^{-0.5} ,$$

$\rho \approx 10^8 \text{ cm}^{-3}$ $\sigma_v \approx 0.5 \text{ km s}^{-1}$ $\sigma_{\text{nt}} \approx 0.5 \text{ km s}^{-1}$ $\langle B_t^2 \rangle / \langle B^2 \rangle \approx 0.5$

with

$$1 - \langle \Delta \Phi(l) \rangle = a_2 l^2 + \frac{\langle B_t^2 \rangle}{\langle B^2 \rangle} C \times \left\{ \frac{1}{C_1} \left[1 - e^{-l^2/2(l_\delta^2 + 2l_{W1}^2)} \right] + \frac{1}{C_2} \left[1 - e^{-l^2/2(l_\delta^2 + 2l_{W2}^2)} \right] - \frac{2}{C_{12}} \left[1 - e^{-l^2/2(l_\delta^2 + l_{W1}^2 + l_{W2}^2)} \right] \right\},$$

$$\frac{\Delta \Phi(l)}{2\sqrt{2} l_{W2}} = \frac{l, l_{W1}}{\sqrt{2} a_2 l^2}$$

$$l_\delta$$

$$C_1 = \frac{(l_\delta^2 + l_{W1}^2)}{\sqrt{2\pi} l_\delta^3},$$

$$C_2 = \frac{(l_\delta^2 + l_{W2}^2)}{\sqrt{2\pi} l_\delta^3},$$

$$C_{12} = \frac{(l_\delta^2 + l_{W1}^2 + l_{W2}^2)}{\sqrt{2\pi} l_\delta^3},$$

$$C = \left(\frac{1}{C_1} + \frac{1}{C_2} - \frac{2}{C_{12}} \right)^{-1}.$$

where

$\langle B_t^2 \rangle / \langle B^2 \rangle = 0.5$

and

$B = 0.2 \pm 2.8$

and

$B_{3D} = 0.2 \pm 3.5$

and

$M_A = \sigma_{nt} / \sigma_A = 0.6 \pm 0.7$

and

$\lambda = \frac{(M/\Phi_B)}{(M/\Phi_B)_{cr}} = \pi G^{1/2} \left[\frac{3}{2} \left(\frac{3-n}{5-2n} \right) \right]^{1/2} \frac{M}{\Phi_B}$

and

$B = B\pi R^2$

and

$n = 2.5$

and

$\lambda = 1.5 \pm 0.5$

and

$\alpha_{vir,B} = \frac{2E_K + E_B}{|E_G|}$

and

$E_B = \frac{1}{8\pi} B^2 V = \frac{1}{6} B^2 R^3$

and

$\alpha_{vir,B} = 0.0 \pm 0.0$

and

$\alpha_{vir,B} = 0.0 \pm 0.0$

and

$\alpha_{vir,B} = 0.0 \pm 0.0$

and

$\alpha_{vir,B} = 0.0 \pm 0.0$

and

$\alpha_{vir,B} = 0.0 \pm 0.0$

E

Table 2. Magnetic Field Properties at Different Dust Temperatures

T	B_{3D}	σ_A	\mathcal{M}_A	λ	E_B	$\alpha_{\text{vir},B}$
(K)	(mG)	(km s ⁻¹)	(cm ⁻³)	(km s ⁻¹)	(erg)	
20	6.2 ± 3.5	0.37 ± 0.23	1.6 ± 0.7	18 ± 13	$4.2 \pm 4.1 \times 10^{43}$	0.064 ± 0.028
50	3.5 ± 2.0	0.37 ± 0.23	1.6 ± 0.7	10 ± 5	$1.4 \pm 1.3 \times 10^{43}$	0.23 ± 0.10

- Beltrán, M. T., Rivilla, V. M., Cesaroni, R., et al. 2021, A&A, 648, A100, doi: [10.1051/0004-6361/202040121](https://doi.org/10.1051/0004-6361/202040121)
- Beuther, H., Soler, J. D., Vlemmings, W., et al. 2018, A&A, 614, A64, doi: [10.1051/0004-6361/201732378](https://doi.org/10.1051/0004-6361/201732378)
- Chambers, E. T., Jackson, J. M., Rathborne, J. M., & Simon, R. 2009, ApJS, 181, 360, doi: [10.1088/0067-0049/181/2/360](https://doi.org/10.1088/0067-0049/181/2/360)
- Chandrasekhar, S., & Fermi, E. 1953, ApJ, 118, 116, doi: [10.1086/145732](https://doi.org/10.1086/145732)
- Chen, H.-R. V., Zhang, Q., Wright, M. C. H., et al. 2019, ApJ, 875, 24, doi: [10.3847/1538-4357/ab0f3e](https://doi.org/10.3847/1538-4357/ab0f3e)
- Commerçon, B., Hennebelle, P., & Henning, T. 2011, ApJL, 742, L9, doi: [10.1088/2041-8205/742/1/L9](https://doi.org/10.1088/2041-8205/742/1/L9)
- Contreras, Y., Sanhueza, P., Jackson, J. M., et al. 2018, ApJ, 861, 14, doi: [10.3847/1538-4357/aac2ec](https://doi.org/10.3847/1538-4357/aac2ec)
- Cortes, P. C., Le Gouellec, V. J. M., Hull, C. L. H., et al. 2021, ApJ, 907, 94, doi: [10.3847/1538-4357/abcafb](https://doi.org/10.3847/1538-4357/abcafb)
- Cortes, P. C., Girart, J. M., Sanhueza, P., et al. 2024, arXiv e-prints, arXiv:2406.14663, doi: [10.48550/arXiv.2406.14663](https://doi.org/10.48550/arXiv.2406.14663)
- Crutcher, R. M., Nutter, D. J., Ward-Thompson, D., & Kirk, J. M. 2004, ApJ, 600, 279, doi: [10.1086/379705](https://doi.org/10.1086/379705)
- Csengeri, T., Leurini, S., Wyrowski, F., et al. 2016, A&A, 586, A149, doi: [10.1051/0004-6361/201425404](https://doi.org/10.1051/0004-6361/201425404)
- Cunningham, N., Ginsburg, A., Galván-Madrid, R., et al. 2023, A&A, 678, A194, doi: [10.1051/0004-6361/202245429](https://doi.org/10.1051/0004-6361/202245429)
- Cyganowski, C. J., Brogan, C. L., Hunter, T. R., et al. 2017, MNRAS, 468, 3694, doi: [10.1093/mnras/stx043](https://doi.org/10.1093/mnras/stx043)
- Cyganowski, C. J., Ilee, J. D., Brogan, C. L., et al. 2022, ApJL, 931, L31, doi: [10.3847/2041-8213/ac69ca](https://doi.org/10.3847/2041-8213/ac69ca)
- Cyganowski, C. J., Brogan, C. L., Hunter, T. R., et al. 2014, ApJL, 796, L2, doi: [10.1088/2041-8205/796/1/L2](https://doi.org/10.1088/2041-8205/796/1/L2)
- Davis, L. 1951, Physical Review, 81, 890, doi: [10.1103/PhysRev.81.890.2](https://doi.org/10.1103/PhysRev.81.890.2)
- Feng, S., Beuther, H., Zhang, Q., et al. 2016, ApJ, 828, 100, doi: [10.3847/0004-637X/828/2/100](https://doi.org/10.3847/0004-637X/828/2/100)
- Fernández-López, M., Girart, J. M., López-Vázquez, J. A., et al. 2023, ApJ, 956, 82, doi: [10.3847/1538-4357/ace786](https://doi.org/10.3847/1538-4357/ace786)
- Fernández-López, M., Sanhueza, P., Zapata, L. A., et al. 2021, arXiv e-prints, arXiv:2104.03331, <https://arxiv.org/abs/2104.03331>
- Guzmán, A. E., Sanhueza, P., Zapata, L., Garay, G., & Rodríguez, L. F. 2020, ApJ, 904, 77, doi: [10.3847/1538-4357/abbe09](https://doi.org/10.3847/1538-4357/abbe09)
- Houde, M., Hull, C. L. H., Plambeck, R. L., Vaillancourt, J. E., & Hildebrand, R. H. 2016, ApJ, 820, 38, doi: [10.3847/0004-637X/820/1/38](https://doi.org/10.3847/0004-637X/820/1/38)
- Houde, M., Vaillancourt, J. E., Hildebrand, R. H., Chitsazzadeh, S., & Kirby, L. 2009, ApJ, 706, 1504, doi: [10.1088/0004-637X/706/2/1504](https://doi.org/10.1088/0004-637X/706/2/1504)
- Ilee, J. D., Cyganowski, C. J., Brogan, C. L., et al. 2018, ApJL, 869, L24, doi: [10.3847/2041-8213/aaeffc](https://doi.org/10.3847/2041-8213/aaeffc)
- Ilee, J. D., Cyganowski, C. J., Nazari, P., et al. 2016, MNRAS, 462, 4386, doi: [10.1093/mnras/stw1912](https://doi.org/10.1093/mnras/stw1912)
- Ishihara, K., Sanhueza, P., Nakamura, F., et al. 2024, arXiv e-prints, arXiv:2407.06845, doi: [10.48550/arXiv.2407.06845](https://doi.org/10.48550/arXiv.2407.06845)
- Izquierdo, A. F., Galván-Madrid, R., Maud, L. T., et al. 2018, MNRAS, 478, 2505, doi: [10.1093/mnras/sty1096](https://doi.org/10.1093/mnras/sty1096)
- Kirk, H., Myers, P. C., Bourke, T. L., et al. 2013, ApJ, 766, 115, doi: [10.1088/0004-637X/766/2/115](https://doi.org/10.1088/0004-637X/766/2/115)
- Krumholz, M. R., Klein, R. I., McKee, C. F., Offner, S. S. R., & Cunningham, A. J. 2009, Science, 323, 754, doi: [10.1126/science.1165857](https://doi.org/10.1126/science.1165857)
- Li, S., Zhang, Q., Pillai, T., et al. 2019, ApJ, 886, 130, doi: [10.3847/1538-4357/ab464e](https://doi.org/10.3847/1538-4357/ab464e)
- Li, S., Sanhueza, P., Zhang, Q., et al. 2020, ApJ, 903, 119, doi: [10.3847/1538-4357/abb81f](https://doi.org/10.3847/1538-4357/abb81f)
- . 2023, ApJ, 949, 109, doi: [10.3847/1538-4357/acc58f](https://doi.org/10.3847/1538-4357/acc58f)
- Li, S., Sanhueza, P., Beuther, H., et al. 2024, Nature Astronomy, 8, 472, doi: [10.1038/s41550-023-02181-9](https://doi.org/10.1038/s41550-023-02181-9)
- Liu, H. B., Galván-Madrid, R., Jiménez-Serra, I., et al. 2015, ApJ, 804, 37, doi: [10.1088/0004-637X/804/1/37](https://doi.org/10.1088/0004-637X/804/1/37)
- Liu, J., Qiu, K., & Zhang, Q. 2022a, ApJ, 925, 30, doi: [10.3847/1538-4357/ac3911](https://doi.org/10.3847/1538-4357/ac3911)
- Liu, J., Zhang, Q., Commerçon, B., et al. 2021, ApJ, 919, 79, doi: [10.3847/1538-4357/ac0cec](https://doi.org/10.3847/1538-4357/ac0cec)

- Liu, J., Zhang, Q., & Qiu, K. 2022b, *Frontiers in Astronomy and Space Sciences*, 9, 943556, doi: [10.3389/fspas.2022.943556](https://doi.org/10.3389/fspas.2022.943556)
- Liu, J., Zhang, Q., Qiu, K., et al. 2020, *ApJ*, 895, 142, doi: [10.3847/1538-4357/ab9087](https://doi.org/10.3847/1538-4357/ab9087)
- Liu, J., Zhang, Q., Lin, Y., et al. 2024, *ApJ*, 966, 120, doi: [10.3847/1538-4357/ad3105](https://doi.org/10.3847/1538-4357/ad3105)
- Liu, T., Lacy, J., Li, P. S., et al. 2017, *ApJ*, 849, 25, doi: [10.3847/1538-4357/aa8d73](https://doi.org/10.3847/1538-4357/aa8d73)
- Machida, M. N., Tomisaka, K., Matsumoto, T., & Inutsuka, S.-i. 2008, *ApJ*, 677, 327, doi: [10.1086/529133](https://doi.org/10.1086/529133)
- Mai, X., Liu, T., Liu, X., et al. 2024, *ApJL*, 961, L35, doi: [10.3847/2041-8213/ad19c3](https://doi.org/10.3847/2041-8213/ad19c3)
- McMullin, J. P., Waters, B., Schiebel, D., Young, W., & Golap, K. 2007, in *Astronomical Society of the Pacific Conference Series*, Vol. 376, *Astronomical Data Analysis Software and Systems XVI*, ed. R. A. Shaw, F. Hill, & D. J. Bell, 127
- Mignon-Risse, R., González, M., & Commerçon, B. 2023, *A&A*, 673, A134, doi: [10.1051/0004-6361/202345845](https://doi.org/10.1051/0004-6361/202345845)
- Mignon-Risse, R., González, M., Commerçon, B., & Rosdahl, J. 2021, *A&A*, 652, A69, doi: [10.1051/0004-6361/202140617](https://doi.org/10.1051/0004-6361/202140617)
- Molet, J., Brouillet, N., Nony, T., et al. 2019, *A&A*, 626, A132, doi: [10.1051/0004-6361/201935497](https://doi.org/10.1051/0004-6361/201935497)
- Morii, K., Sanhueza, P., Nakamura, F., et al. 2021, *ApJ*, 923, 147, doi: [10.3847/1538-4357/ac2365](https://doi.org/10.3847/1538-4357/ac2365)
- . 2023, *ApJ*, 950, 148, doi: [10.3847/1538-4357/accea](https://doi.org/10.3847/1538-4357/accea)
- Morii, K., Sanhueza, P., Zhang, Q., et al. 2024, *ApJ*, 966, 171, doi: [10.3847/1538-4357/ad32d0](https://doi.org/10.3847/1538-4357/ad32d0)
- Moscadelli, L., Sánchez-Monge, Á., Goddi, C., et al. 2016, *A&A*, 585, A71, doi: [10.1051/0004-6361/201526238](https://doi.org/10.1051/0004-6361/201526238)
- Myers, A. T., McKee, C. F., Cunningham, A. J., Klein, R. I., & Krumholz, M. R. 2013, *ApJ*, 766, 97, doi: [10.1088/0004-637X/766/2/97](https://doi.org/10.1088/0004-637X/766/2/97)
- Nony, T., Louvet, F., Motte, F., et al. 2018, *A&A*, 618, L5, doi: [10.1051/0004-6361/201833863](https://doi.org/10.1051/0004-6361/201833863)
- Offner, S. S. R., Moe, M., Kratter, K. M., et al. 2023, in *Astronomical Society of the Pacific Conference Series*, Vol. 534, *Protostars and Planets VII*, ed. S. Inutsuka, Y. Aikawa, T. Muto, K. Tomida, & M. Tamura, 275, doi: [10.48550/arXiv.2203.10066](https://doi.org/10.48550/arXiv.2203.10066)
- Ohashi, S., Sanhueza, P., Chen, H.-R. V., et al. 2016, *ApJ*, 833, 209, doi: [10.3847/1538-4357/833/2/209](https://doi.org/10.3847/1538-4357/833/2/209)
- Olguin, F. A., Sanhueza, P., Ginsburg, A., et al. 2022, *ApJ*, 929, 68, doi: [10.3847/1538-4357/ac5bd8](https://doi.org/10.3847/1538-4357/ac5bd8)
- Olguin, F. A., Sanhueza, P., Guzmán, A. E., et al. 2021, *ApJ*, 909, 199, doi: [10.3847/1538-4357/abde3f](https://doi.org/10.3847/1538-4357/abde3f)
- Olguin, F. A., Sanhueza, P., Chen, H.-R. V., et al. 2023, *ApJL*, 959, L31, doi: [10.3847/2041-8213/ad1100](https://doi.org/10.3847/2041-8213/ad1100)
- Ossenkopf, V., & Henning, T. 1994, *A&A*, 291, 943
- Peretto, N., Fuller, G. A., André, P., et al. 2014, *A&A*, 561, A83, doi: [10.1051/0004-6361/201322172](https://doi.org/10.1051/0004-6361/201322172)
- Pillai, T., Kauffmann, J., Zhang, Q., et al. 2019, *A&A*, 622, A54, doi: [10.1051/0004-6361/201732570](https://doi.org/10.1051/0004-6361/201732570)
- Rathborne, J. M., Jackson, J. M., & Simon, R. 2006, *ApJ*, 641, 389, doi: [10.1086/500423](https://doi.org/10.1086/500423)
- Redaelli, E., Bovino, S., Sanhueza, P., et al. 2022, *arXiv e-prints*, arXiv:2208.01675, <https://arxiv.org/abs/2208.01675>
- Rosolowsky, E. W., Pineda, J. E., Kauffmann, J., & Goodman, A. A. 2008, *ApJ*, 679, 1338, doi: [10.1086/587685](https://doi.org/10.1086/587685)
- Saha, P., Sanhueza, P., Padovani, M., et al. 2024, *arXiv e-prints*, arXiv:2407.16654, doi: [10.48550/arXiv.2407.16654](https://doi.org/10.48550/arXiv.2407.16654)
- Sanhueza, P., Jackson, J. M., Foster, J. B., et al. 2012, *ApJ*, 756, 60, doi: [10.1088/0004-637X/756/1/60](https://doi.org/10.1088/0004-637X/756/1/60)
- . 2013, *ApJ*, 773, 123, doi: [10.1088/0004-637X/773/2/123](https://doi.org/10.1088/0004-637X/773/2/123)
- Sanhueza, P., Jackson, J. M., Zhang, Q., et al. 2017, *ApJ*, 841, 97, doi: [10.3847/1538-4357/aa6ff8](https://doi.org/10.3847/1538-4357/aa6ff8)
- Sanhueza, P., Contreras, Y., Wu, B., et al. 2019, *ApJ*, 886, 102, doi: [10.3847/1538-4357/ab45e9](https://doi.org/10.3847/1538-4357/ab45e9)
- Sanhueza, P., Girart, J. M., Padovani, M., et al. 2021, *ApJL*, 915, L10, doi: [10.3847/2041-8213/ac081c](https://doi.org/10.3847/2041-8213/ac081c)
- Sato, M., Wu, Y. W., Immer, K., et al. 2014, *ApJ*, 793, 72, doi: [10.1088/0004-637X/793/2/72](https://doi.org/10.1088/0004-637X/793/2/72)
- Silva, A., Zhang, Q., Sanhueza, P., et al. 2017, *ApJ*, 847, 87, doi: [10.3847/1538-4357/aa88c6](https://doi.org/10.3847/1538-4357/aa88c6)
- Tan, J. C., Beltrán, M. T., Caselli, P., et al. 2014, in *Protostars and Planets VI*, ed. H. Beuther, R. S. Klessen, C. P. Dullemond, & T. Henning, 149–172, doi: [10.2458/azu_uapress_9780816531240-ch007](https://doi.org/10.2458/azu_uapress_9780816531240-ch007)
- Tan, J. C., Kong, S., Butler, M. J., Caselli, P., & Fontani, F. 2013, *ApJ*, 779, 96, doi: [10.1088/0004-637X/779/2/96](https://doi.org/10.1088/0004-637X/779/2/96)
- Tan, J. C., Kong, S., Zhang, Y., et al. 2016, *ApJL*, 821, L3, doi: [10.3847/2041-8205/821/1/L3](https://doi.org/10.3847/2041-8205/821/1/L3)
- Tanaka, K. E. I., Zhang, Y., Hirota, T., et al. 2020, *ApJL*, 900, L2, doi: [10.3847/2041-8213/abadfc](https://doi.org/10.3847/2041-8213/abadfc)
- Taniguchi, K., Sanhueza, P., Olguin, F. A., et al. 2023, *ApJ*, 950, 57, doi: [10.3847/1538-4357/acca1d](https://doi.org/10.3847/1538-4357/acca1d)
- Tsuribe, T., & Inutsuka, S.-i. 1999, *ApJ*, 526, 307, doi: [10.1086/307983](https://doi.org/10.1086/307983)
- Vaillancourt, J. E. 2006, *PASP*, 118, 1340, doi: [10.1086/507472](https://doi.org/10.1086/507472)
- Wang, K., Zhang, Q., Testi, L., et al. 2014, *MNRAS*, 439, 3275, doi: [10.1093/mnras/stu127](https://doi.org/10.1093/mnras/stu127)
- Wells, M. R. A., Beuther, H., Molinari, S., et al. 2024, *arXiv e-prints*, arXiv:2408.08299, doi: [10.48550/arXiv.2408.08299](https://doi.org/10.48550/arXiv.2408.08299)

Xu, F.-W., Wang, K., Liu, T., et al. 2023, MNRAS, 520, 3259, doi: [10.1093/mnras/stad012](https://doi.org/10.1093/mnras/stad012)

Zapata, L. A., Fernández-López, M., Sanhueza, P., et al. 2024, arXiv e-prints, arXiv:2408.10199, doi: [10.48550/arXiv.2408.10199](https://doi.org/10.48550/arXiv.2408.10199)

Zhang, Q., Wang, Y., Pillai, T., & Rathborne, J. 2009, ApJ, 696, 268, doi: [10.1088/0004-637X/696/1/268](https://doi.org/10.1088/0004-637X/696/1/268)

Zhang, S., Cyganowski, C. J., Henshaw, J. D., et al. 2024, MNRAS, 533, 1075, doi: [10.1093/mnras/stae1844](https://doi.org/10.1093/mnras/stae1844)

Zhang, Y., Tan, J. C., Tanaka, K. E. I., et al. 2019, Nature Astronomy, 3, 517, doi: [10.1038/s41550-019-0718-y](https://doi.org/10.1038/s41550-019-0718-y)